Forest Canopy Height Extraction in Rugged Areas With ICESat/GLAS Data

Xiaoyi Wang, Huabing Huang, Peng Gong, Caixia Liu, Congcong Li, and Wenyu Li

***Abstract*—Geoscience Laser Altimeter System data have been widely used in forest canopy height extraction. It is still challenging over rugged areas. In this paper, we propose a forest canopy height extraction method consisting of the Savitzky–Golay filter and fitting, Sigbeg determination based on the fitting results, and slope correction for rugged areas, particularly for slopes ranging from 5° to 15°. The method was applied to both the Xinlin Forest, China, and Santa Rosa National Park, Costa Rica. The performance of this method was validated by field measurement and Laser Vegetation Imaging Sensor data. The goodness of fit (R^2) reached 0.73 and 0.78, respectively, and root-mean-squared errors (RMSEs) were 2.27 and 3.75 m over the two areas, respectively.**

***Index Terms*—Forest inventory, global forest monitoring.**

I. Introduction

FOREST canopy height is an important structural parameter in forest inventory and helpful to the understanding of forest ecosystem function and modeling of terrestrial carbon cycling [1], [2]. The Geoscience Laser Altimeter System (GLAS) onboard the National Aeronautics and Space Administration (NASA) Ice, Cloud, and land Elevation satellite (ICESat) is the only direct measurement sensor that can provide fast tree height solutions at the global scale [3], [4]. However, the accuracy of the resulting tree heights is affected by terrain slope and roughness [5].

The beam of GLAS covers an area of approximately 65 m in diameter and records the reflection waveform of aboveground objects and ground surface, consisting of a series of discrete sampling points with multiple peaks. NASA provides users with land surface altimetry product, GLA14, derived from GLAS raw waveforms. The widely accepted procedure for canopy height extraction is as follows.

Initially, a waveform is filtered with a Gaussian filter, and the width of the filter is almost the same as the transmitted waveform. After that, the "Signal beginning point" (Sigbeg), which stands for the tree top, is defined as the point which goes beyond the threshold. Then, discrete sampling points are expressed as the sum of multiple Gaussian waves through Gaussian decomposition, and the last Gaussian wave peak representing the ground surface could be determined. Eventually, the tree extraction is calculated by the vertical distance between Sigbeg and the last Gaussian peak.

Studies have shown that the last Gaussian wave peak may be caused by small trees [6] or noises and does not stand for the ground return. Some improvements have been made to choose the stronger one among the last two Gaussian decomposition results [7]. Whereas the chosen peak may not be able to represent ground without proper noise reduction, there have been some improvements of waveform denoising. Wu [8] and Wang [9] introduced the wavelet transform method. However, with the appropriate widow size and threshold changing with different situations, it is difficult to obtain unified parameters suitable for large areas.

The threshold to define Sigbeg is calculated as the mean background noise value plus N times of noise standard derivation (std), while the result is linked closely to the background noise information given by GLA05 (i.e., the mean and standard derivation of noise), and the choice of noise standard derivation coefficient N varies with each study. Chen [6] reports that the most suitable N to predict vegetation height differs at different sites and is not constantly affected by background noise. To our knowledge, all existing Sigbeg determination methods rely on predefined empirical thresholds of noises while completely ignoring the information from the waveform distribution. There has only been a paucity of research about Sigbeg calculation based on GLAS waveform [8], [10].

The processes and improved methods mentioned earlier are insufficient over rugged areas, while slope correction (SC) is needed. Despite the difficulties in SC, efforts have been undertaken to reduce the influence of the slope. Lefsky *et al.* [11] established the relationship between canopy extraction and waveform parameters (waveform extent, leading edge extent, and trailing edge extent) or waveform extent and ancillary digital elevation model (DEM) [12] with multiple regression, but the height extraction when applied at the global scale appears problematic [4], [13]. Pang *et al.* [14] set up the regression between waveform parameters and crown-area-weighted height.

Manuscript received February 13, 2013; revised July 14, 2013; accepted September 16, 2013. This work was supported in part by a National High Technology Grant of China (2009AA12200101).

X. Wang, C. Liu, and W. Li are with the State Key Laboratory of Remote Sensing Science, Jointly Sponsored by the Institute of Remote Sensing and Digital Earth, Chinese Academy of Sciences (CAS) and Beijing Normal University, Beijing 100101, China, and also with the University of the Chinese Academy of Sciences, Beijing 100049, China.

H. Huang is with the State Key Laboratory of Remote Sensing Science, Jointly Sponsored by the Institute of Remote Sensing and Digital Earth, CAS and Beijing Normal University, Beijing 100101, China.

P. Gong is with the State Key Laboratory of Remote Sensing Science, Jointly Sponsored by the Institute of Remote Sensing and Digital Earth, CAS and Beijing Normal University, Beijing 100101, China. He is also with the Ministry of Education Key Laboratory for Earth System Modeling, Center for Earth System Science, Tsinghua University, Beijing 100084, China, and also with the Department of Environmental Science, Policy and Management, University of California, Berkeley, Berkeley, CA 94720, USA (e-mail: penggong@berkeley.edu).

C. Li is with the College of Global Change and Earth System Science, Beijing Normal University, Beijing 100875, China.

Color versions of one or more of the figures in this paper are available online at http://ieeexplore.ieee.org.

Digital Object Identifier 10.1109/TGRS.2013.2283272

While those methods are essentially site specific, the results depend on the quantity and accuracy of field measured data. Lee *et al.* [15] removed the slope effect with approximate geometric correction. The correction eliminates the slope influence of the footprint center, and the calculated result relies on the accuracy of slope estimation.

This research is motivated by the requirement in forest land cover mapping at the global scale [16]. In order to better distinguish forest from shrubs and grasslands, it is desirable to have accurate estimation of tree heights. The objective of this research is to obtain more accurate forest canopy height in rugged areas, particularly for slopes below 15° using GLAS data. We propose a way to improve the height extraction process and further investigate the algorithm of SC calculated from the waveform which is suitable for randomly distributed forests.

II. Study Area and Data

A. Study Area

The research was conducted in the Xinlin Forest and Santa Rosa National Park (SRNP), respectively. Xinlin Forests is the jurisdiction of Daxing'anling Prefecture, located in Heilongjiang Province, China. The area belongs to highland cold temperate continental monsoon climate. The forest is dominated by coniferous forest with a small number of broad-leaved and mixed forests scattering in the lower valleys. This area was rarely affected by large fires and other disturbance, and as a result, much of the forest is composed of mature trees. The topography is widely variable, and according to the measured data, 63.5% of the area has a slope greater than 5°. The slope level of each GLAS footprint was revealed by different color in Fig. 1, and the histogram of the slope illustrated the frequency distribution of slopes. The canopy height ranges from 6 to 19 m, with an average of 12 m.

SRNP is located in the Guanacaste Province in the northeastern Costa Rica. The park was constructed in 1971 to protect the remaining fragments of tropical dry forest. It has ten different habitats, widely attracting all sorts of animals, with the vegetation here including oak forest, mangrove swamp, and savannah. The northern part of this region is relatively flat, while the slope of the southern part could reach 61°. The canopy height ranges from 2.39 to 28.83 m, with an average of 16.05 m.

B. Data Collection

1) GLAS Data: NASA provides 15 GLAS data products (GLA01–GLA15) and supplies users with the surface elevation distribution within each footprint. The near-polar orbit satellites covered between 86° N and 86° S globally with the altitude of approximately 600 km. The footprint diameter is about 65 m, varied in size and shape, and the vertical accuracy could reach 15 cm in areas with low slope [17].

The products used in this study include GLA01, GLA05, and GLA14 from Rlease-33. For the Xinlin site, the GLAS footprints were from the campaign of L3C (May–June 2005), L3D (October–November 2005), L3F (May–June 2006), and L3G (October–November 2006). For the SRNP site, only the campaigns of L3C and L3D were available according to the Laser Vegetation Imaging Sensor (LVIS) data acquisition time. GLA01 provides fully received waveforms with approximate geolocations. GLA05 offers the waveform-based range correction data, and GLA14 contains land surface altimetry with accurate location. To get the full waveform with precise latitude and longitude coordinates and corresponding modification data, the fields of i_UTCTime and i_dShotTime were used to connect these three products.

2) Field Experiment Data: National Forest Management Inventory (NFMI) data were used to evaluate the canopy extraction of the Xinlin Forest. The inventory data were gathered during the year of 2005 and 2006 at subcompartment level, and the time was consistent with the GLAS data. Since only average canopy height was recorded in NFMI data, mature forests (with the age class of V and VI) or relatively uniform growing forests (judged by the visual interpretation of the height and shadow of trees from Google Earth high resolution imagery) were selected to assess the results, whose dominant height (evaluated by GLAS) was close to the average height (collected from inventory data).

3) LVIS Data: Airborne laser altimeter system LVIS data over the SRNP area were provided by the LVIS team in the Laser Remote Sensing Branch at the NASA Goddard Space Flight Center. The LVIS data were acquired in March 2005 with a footprint size of 20 m. The LVIS Ground Elevation product was used, recording the 25%, 50%, 75%, and 100% of cumulative return energy relative to the total energy, and 100% of the waveform energy (RH100) was considered as the treetop height [18]. Since each GLAS footprint embeds 7–9 LVIS shots, the maximum of the RH100 within each GLAS footprint was applied to evaluate the canopy extraction computed from GLAS data.

4) SRTM Data: The Shuttle Radar Topography Mission (SRTM) is an international project spearheaded by the National Geospatial-Intelligence Agency and NASA. It provides users with high-resolution digital topographic data. Three arcsecond (90 m) SRTM3 data from the Consortium for Spatial Information (http://csi.cgiar.org) are available to generate slope data for the SRNP area, and gaps have been filled by using the TOPOGRID algorithm with auxiliary DEM [19]. The data set was processed with the "Slope" function in Arcgis 9.3.

III. Height Extraction Method

A. Waveform Preprocessing

1) Footprint Selection: The footprint was filtered by the parameter i_satCorrFlg recorded in GLA14. If i_satCorrFlg is greater than 2, it indicates waveform saturation, and the corresponding footprint is not considered.

The amplitudes of the GLA01 waveform recorded in raw counts were transformed into volts with a conversion table listed in the file header of the products.

2) Confirming the Rough Range of Useful Information: The rough range of useful information is initially determined by the mean and std of background noise estimation obtained from GLA05, and we searched for the first bin that exceeds the threshold of mean $+3^*$ std from both sides. As a result, part of the useless information is removed.

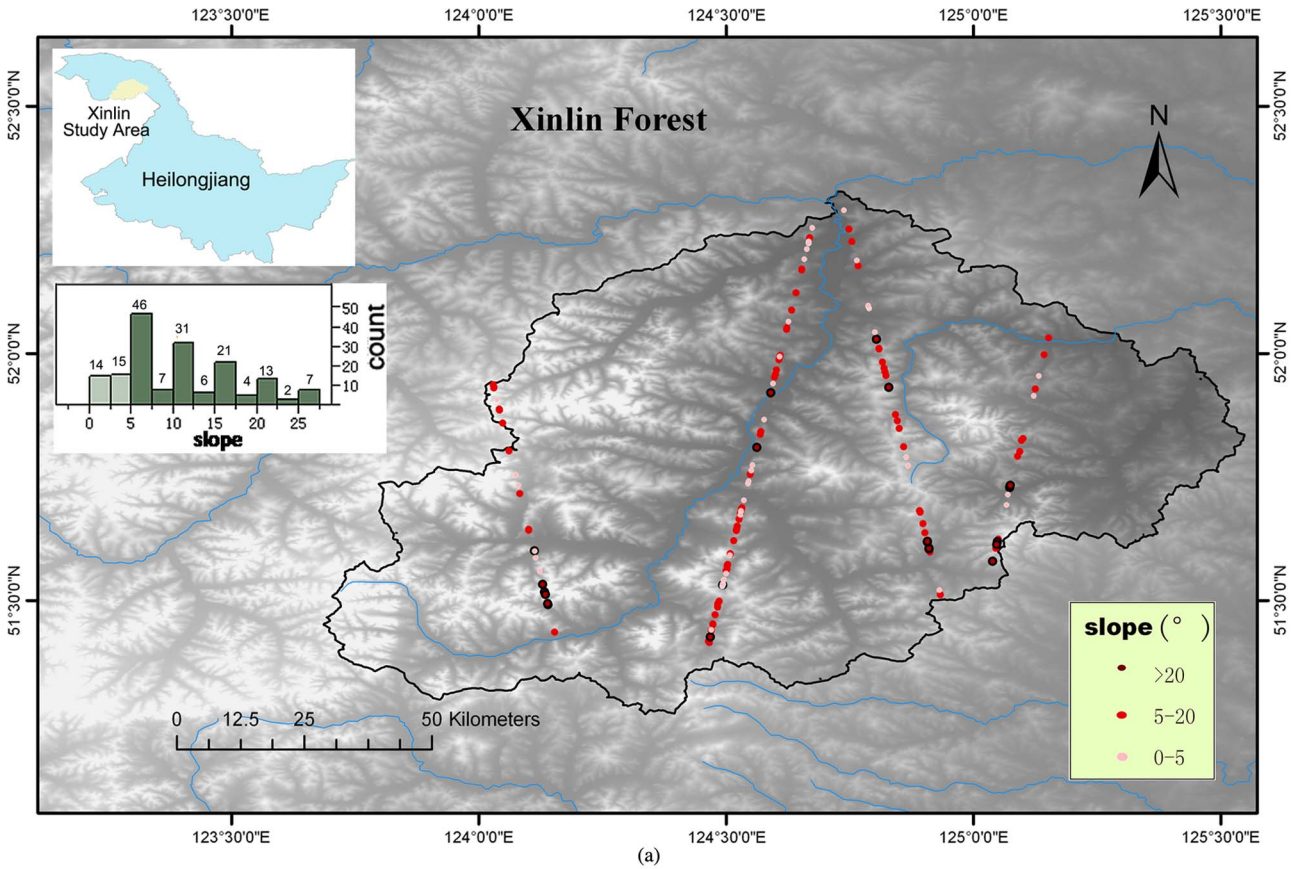

(a)

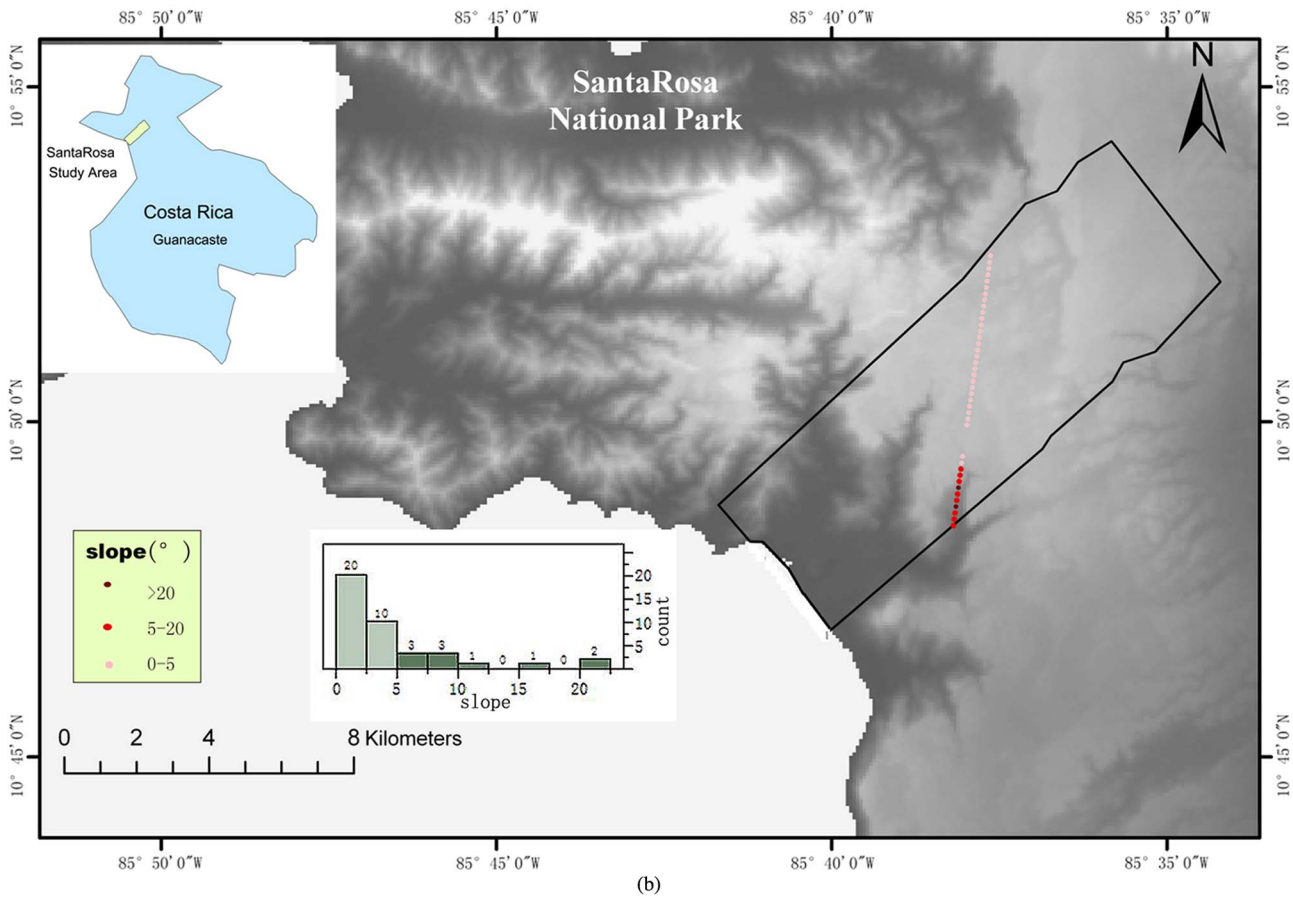

(b)

Fig. 1. Study areas. (a) Xinlin Forest in Heilongjiang Province, China, and (b) SRNP in Guanacaste Province, Costa Rica. The points indicate locations and slope level of GLAS data.

B. Waveform Decomposition

1) Noise Reduction With SG Filter: The Savitzky–Golay (SG) filter has been put forward as a polynomial least squares fitting within a filter window [20]. The window selects part or the whole of the signal and calculates the weighted average with certain degree of polynomial weighting. The weighting is designed to keep higher moments of the data and cut down the bias caused by the filter. Chen [21] has indicated that this filter deals well with narrow peaks. The heights and widths of the waveform are quite extraordinarily preserved, at the cost of not reducing as much noise as a low-pass filter.

Here, a global filter is utilized to further reduce the influence of noise, and the equation of the polynomial least squares fitting for the waveform can be expressed as follows:

$$Y = \frac{\sum_{i=-m}^{m} C_i X_i}{N} \tag{1}$$

where X_i is the original waveform, Y is the smoothed waveform, N is the number of point participating calculation and equals the size of the waveform, and m equals half of the waveform size. C_i stands for the weighting coefficient of the ith point within the filter window, and it satisfies the least squares condition

$$\sum_{i=-m}^{m} [Y(X_i - X_i)]^2 = \min . \tag{2}$$

Savitzky and Golay listed the coefficients, and they were corrected by Steinier *et al.* [22], which can be used directly.

2) Waveform Fitting: Waveform fitting was processed by applying the method in [23]. Two inflection points are first calculated to determine each Gaussian waveform, and the Trust Region Reflective algorithm is repeated to reach an effective fitting result.

C. Sigbeg Determination

We define Sigbeg to be independent of noise estimation and experimental trials of parameter N. In view of Gaussian decomposition results, the Sigbeg point is identified based on the normal cumulative distribution function $\phi(x)$, which can completely describe the probability distribution of random variable "signal time" and could find the probability $P(x)$ whose signal time with a normal distribution at a value is less than or equal to a specific "signal time"

$$P(\mu - k\sigma < x < \mu + k\sigma) = 2\phi(k) - 1 \tag{3}$$

$$\phi(x) = \frac{1}{\sqrt{2\pi}} \int_{-\infty}^{x} e^{\frac{1}{2}t^2} dt \tag{4}$$

where $t = (x - \mu/\sigma)$, μ and σ stand for the estimated mean and standard derivation of the first Gaussian decomposition result. From (3) and (4), 99.73% of the signal information within the interval of $\mu \pm 3\sigma$ would be retained [24]. As a

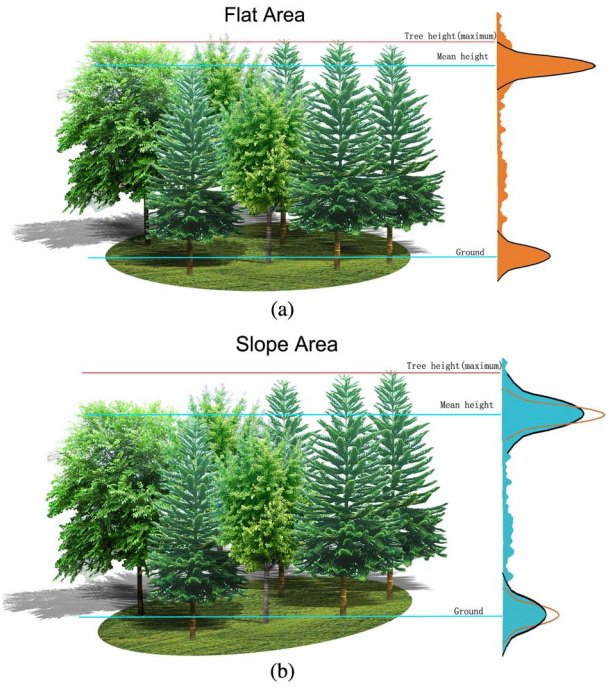

Fig. 2. Three-dimensional scenes of flat area and rugged area. (a) Received waveform from flat area and the variance of ground peak. (b) Received waveform from rugged area and the broadened variance of ground peak.

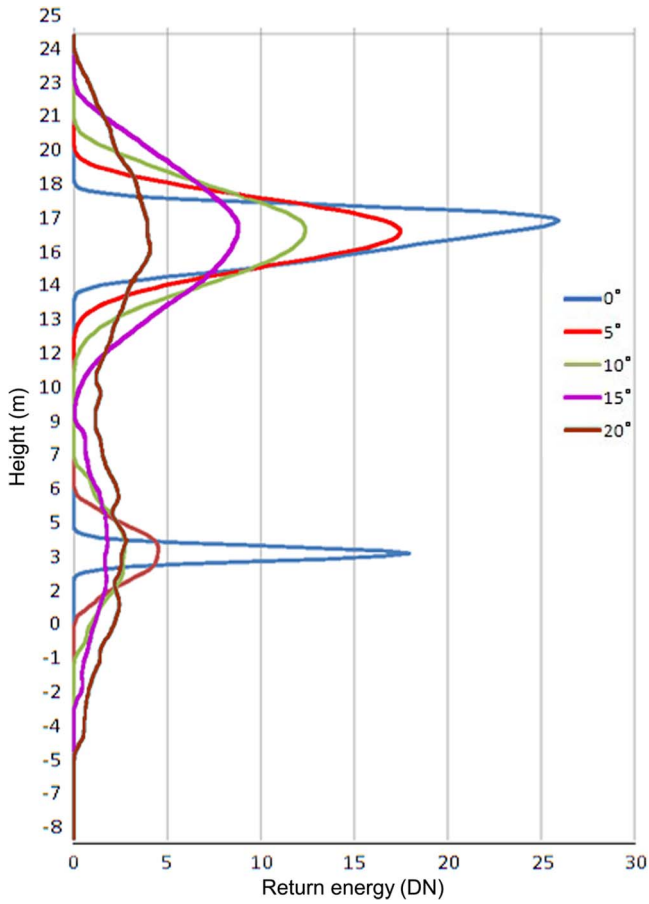

Fig. 3. Model simulation results. Trees are distributed randomly with the height of 20 m, and the shape is an ellipsoid or cone. Waveform over 5°, 10°, and 15° in slope could be restored to the line of 0°. The peak of canopy and ground merged with slope of 20°.

TABLE I
WAVEFORM WAS BROADENED FOR CANOPY AND GROUND IN RUGGED AREA. THE SIMULATION WAS REPEATED 300 TIMES WITH DIFFERENT COVERAGE RANGING FROM 10% TO 90%

		variance estimated by 3σ (bins)						
		0°	5°	broaden	10°	broaden	15°	broaden
20m	canopy	28.0±0.00	40.6±0.55	12.6±0.55	56.2±1.00	28.2±1.09	67.8±1.30	39.8±1.30
	ground	15.0±0.00	29.0±0.00	14.0±0.00	45.0±0.00	30.0±0.00	58.0±0.00	43.0±0.00
15m	canopy	24.0±0.71	36.6±0.89	12.6±0.55	53.8±2.77	29.8±2.86	65.0±2.12	41.0±2.24
	ground	15.0±0.00	29.0±0.00	14.0±0.00	46.0±0.00	31.0±0.00	58.0±0.00	43.0±0.00

result, signal time $T < \mu - 3\sigma$ could be discarded, with little possibility of occurrence and negligible loss of information. Sigbeg estimated in this research could be searched as the point where Sigbeg_$3\sigma = \mu - 3\sigma$.

D. SC

When a laser beam interacts with a flat surface, the variance of the received waveform is the same as that of the transmitted waveform recorded in GLA01 [shown in Fig. 2(a)]. With the increase of the slope gradient, the variance of the received waveform broadens accordingly [5]. While the laser beam interacts with natural growing trees that are randomly distributed, the distance between the centroid of the first and the last peak will represent the trees' mean height. As terrain slope and roughness increase, the waveform distance standing for the mean height would remain the same, while the variance of the received waveform of trees and ground would increase in a similar number of bins [see Fig. 2(b)] [25]. Here, the variance of each decomposed Gaussian waveform was calculated as three times the standard derivation. Fig. 3 and Table I show the simulation results using the 3-D model [26], [27] which illustrates the aforementioned statement.

Three-dimensional scenes were put into the model by assuming that trees are distributed randomly with a height of 20 m, and the shape of the canopy was set as an ellipsoid for deciduous trees and as a cone for conifer trees. The model was parameterized using simulated forest stand attributes from [26, Table II(b)] with different descriptions for deciduous and conifer trees. Transmitted laser was assumed in 5-ns duration of Gaussian shape, and the received laser was digitalized in 1 ns according to the resolution of ICESat/GLAS data (see Table I).

Fig. 3 illustrates the simulation results with a tree coverage of 40%. It also reveals that the waveform of the canopy and ground can be distinguished for slopes of 15° or less. When the slope increases furthermore, the ground and canopy peaks would gradually merge. When the slope increases to 20°, it would cause difficulty in height extraction.

Based on the aforementioned theory, the difference between the variance of the last Gaussian waveform (stands for the ground) and transmit waveform (recorded in GLA01) was considered as being caused by the slope. The slope effect on canopy extraction was reduced by obtaining the correct Sigbeg with the method of compressing the first Gaussian waveform (represents the canopy) from the "broadened waveform" while keeping the centroid of each part unchanged. The Sigbeg point could be restored from $\text{Sigbeg}_{\text{slope}}$ correctly. The correction was achieved with

$$\text{Sigbeg} = \text{Sigbeg}_{\text{slope}} - 3 \times (\sigma_{\text{last\_peak}} - \sigma_{\text{transmit}}). \quad (5)$$

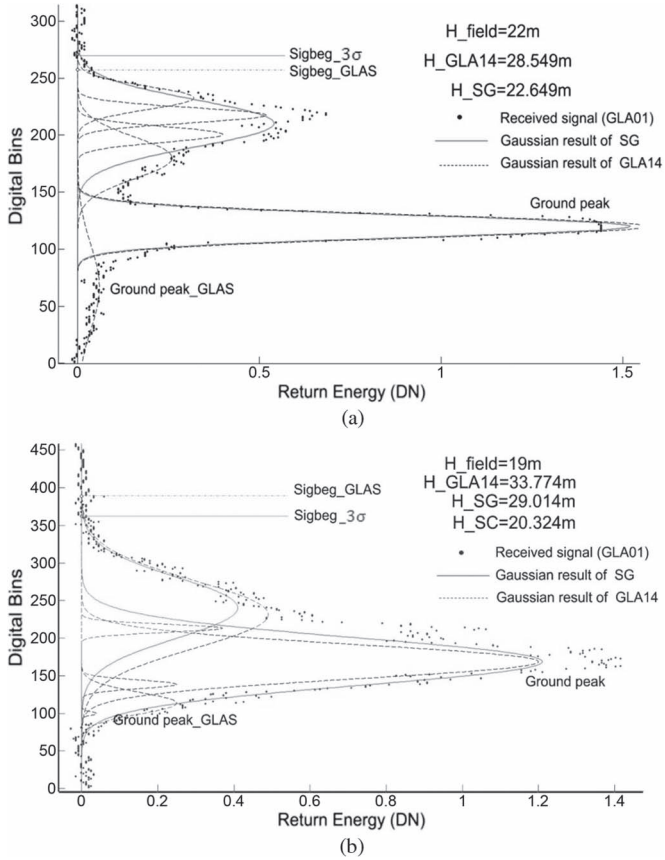

Fig. 4. ICESat/GLAS waveform in the study area. In both Fig. 4(a) and (b), the dots represent sampled waveform from GLA01. The dashed curves show the fitting results recorded in GLA14, and the solid curves describe the result calculated in this research. The dashed lines mark the Sigbeg_GLAS noted in GLA14, while the solid lines mark the Sigbeg_3σ estimated with the method presented earlier. Ground peak_GLAS and Ground peak indicate the ground return results of GLA14 and the results using the SG filter before waveform fitting, respectively.

IV. RESULTS

Waveform decomposition results in this research and the GLA14 were shown in Fig 4. Comparing Sigbeg_3σ and Sigbeg_GLAS of Fig. 4(a) and (b), it can be found that the relative value of Sigbeg_3σ was fixed which describes the signal beginning point properly, while the relative value of Sigbeg_GLAS varied. Since Sigbeg_GLAS was calculated by

using $mean + 4.5^{*}std$ of the noise, the result was influenced by noise, particularly for the singular value in Fig. 4(b). The trail of different N, which equaled 4.5 for the GLA14 of version 33, 4.5 for Simard *et al.* [4] and Lefsky *et al.* [11], 4 for Lefsky *et al.* [12], and 3 for Sun *et al.* [25], would face similar problems, and the relative value swung for different waveforms.

The ground peak of GLA14 was affected by noise as well, and the last peak does not stand for ground in both Fig. 4(a) and (b). In Fig. 4(b), the real ground corresponds to four peaks in GLA14 results. Although the improved method of choosing the stronger one among the last two Gaussian decomposition peaks was suitable for Fig. 4(a), it still missed the ground for Fig. 4(b). The fitting results with SG filtering in this research could properly reduce the noise and preserve the shape of the waveform. While it might still ignore some detailed information, it is not suitable for multilayer building height extraction.

In Fig. 4(b), the slope of the footprint calculated from SRTM data is 19.6°, as a result the ground waveform was broadened. The canopy height in GLA14 (H_GLA14) was 33.774 m, and the SG filtering result without SC (H_SG) was 29.014 m. The canopy height was overestimated owing to the influence of the slope. After SC, the result (H_SC) was 20.324 m which was closer to the field data, 19 m. Since the slope is relatively large, the peaks of canopy and ground are merged which may introduce some errors.

R^2 is a frequently used measure of goodness of fit. The root-mean-squared error (RMSE) is used to describe the differences between values estimated (canopy height extracted in this research) and values actually observed. The algorithm aforementioned was applied to 166 footprints over the Xinlin Forest area, and 119 footprints were from the rugged area with slopes above 5°. The goodness of fit (R^2) with the aforementioned method was 0.73, and the RMSE was 2.27 m as shown in Fig 5(a). The regression line revealed that the results with our method fit well with the field data. Since the inventory data were recorded in integer numbers, it was shown relatively gathered. Owing to the random tree distribution, the results in rugged areas were good (see Table II). RMSE increased when the slope became steeper. At lower than 15° slopes, RMSE remained relatively stable. However, there was a significant rise when the slope exceeded 15°. The canopy peak would merge with the ground peak, making it difficult to extract tree height. Seven footprints with relatively low accuracy were marked by red stars, and they all have greater than 15° slopes.

Four footprints marked with purple stars also had low accuracies, and they were distributed at the border of the forest. The SC may overestimate the height when trees gathered on the upper portion of the footprints along the slope since the peak of canopy waveforms would move upward with the increase of the slope. Conversely, it may underestimate the height when trees gather at the lower portion of the footprints along the slope.

The regression line for the SRNP area includes 39 footprints. The goodness of fit (R^2) with our method is 0.78, and the RMSE is 3.01 m as shown in Fig 5(b). In this area, SRTM data were used to calculate the slope within each footprint. There are eight footprints located on slopes ranging from 5° to 15°, and their canopy heights range from 12.62 to 28.83 m. The RMSE of these footprints is 3.75 m. In the flat area with less than

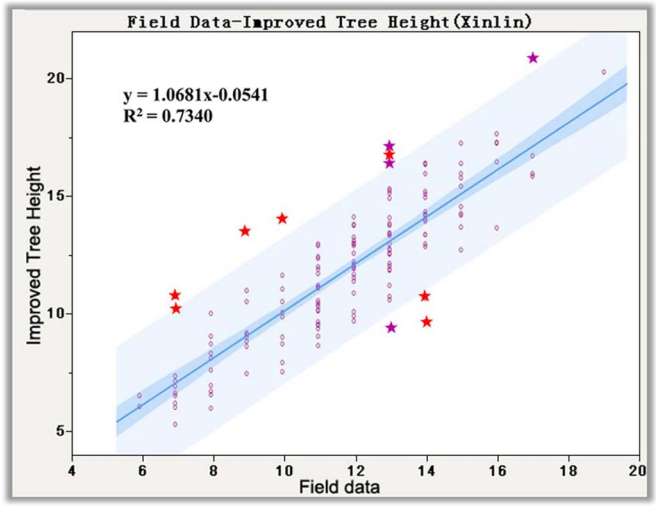

(a)

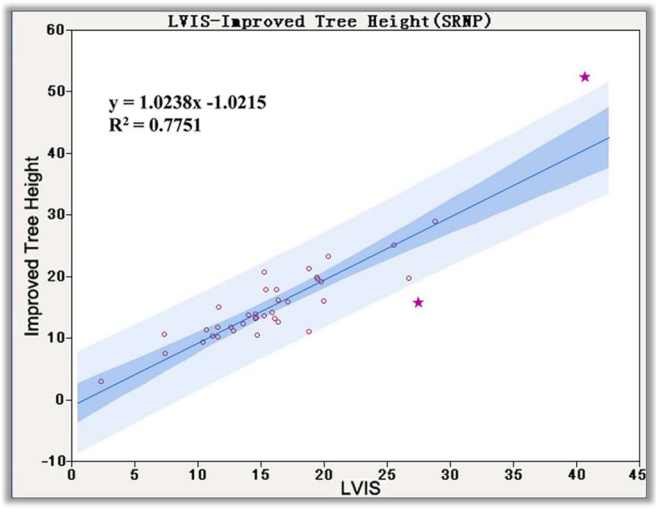

(b)

Fig. 5. Scatterplot of improved tree height extraction versus field data and LVIS data for Xinlin area and SRNP, respectively. Dark blue represents the 95% confidence intervals for the regression line, and light blue represents the 95% prediction intervals for individual observations.

5° slopes, there were 29 footprints, and their RSME was only 2.34 m. This indicates that the method is also applicable to flat areas. Two footprints with low accuracies were marked by purple stars whose slopes were greater than 20°.

The fitting statistics of different slope levels were represented in Table III. Since there were no sufficient data for slopes exceeding 15°, the results were not shown in the table. The second row in Table III depicted the variation of fitting statistics when Sigbeg_3σ of improved result (in the first row) was replaced by Sigbeg_GLAS, R^2 decreased from 0.78 to 0.70, and RMSE increased from 3.01 to 3.69 m. It can be found that the calculation of the Sigbeg played an important role in height extraction. As a comparison, the results of GLA14, Lefsky, and Lee were shown in the table. Lee's result [15] can be computed as follows:

$$H\_\text{Lee} = H\_\text{GLA14} - \frac{65}{2} \times \tan(\text{slope}) \tag{6}$$

and the diameter of the footprint was set to 65 m. Lefsky's result [3] was calculated using the equation of broadleaf.

TABLE II
ACCURACY FOR DIFFERENT SLOPE LEVEL IN XINLIN AREA

	R^2	RMSE(m)	RMSE(0°-5°) (m)	RMSE(5°-15°) (m)	RMSE(15°-20°) (m)	RMSE(>20°) (m)
Improved	0.73	2.27	1.27	2.12	4.05	4.13

TABLE III
COMPARISON BETWEEN RESULTS IN THIS RESEARCH AND OTHERS

	R^2	RMSE(m)	RMSE(0°-5°) (m)	RMSE(5°-15°) (m)
Improved	0.78	3.01	2.34	3.75
Improved (Sigbeg _GLAS)	0.70	3.69	2.63	5.93
Lee	0.59	5.46	4.10	7.96
Lefsky	0.53	3.36	2.34	4.79
GLA14	0.70	6.44	4.07	10.00

As shown in Table III, the improved canopy height outperforms all others with the highest R^2 and lowest RMSE. Lee's result may be influenced by the accuracy of slope and footprint size. The global parameter of Lefsky's equation did not perform well for local sites as ours, and the calculated Lorey's height has some difference with the canopy height which can lead to slight bias.

V. CONCLUSIONS AND DISCUSSION

A processing flow of GLAS data for canopy height extraction over rugged terrains is presented here. Compared with existing methods, our method produced results which are in better agreement with validation data. The method is suitable for canopy height extraction with GLAS data with lower than 15° slopes under a condition of random distribution of trees.

For clustered forests, the method would be influenced if the footprints were located at the border of forests. The inventory data of the Xinlin area were collected only by averaging tree heights of mature forests or uniformly growing forests. This may affect the accuracy of the mean dominant tree height (evaluated by GLAS). More efforts should be made to estimate the applicability of this method.

ACKNOWLEDGMENT

The authors would like to thank the National Snow and Ice Data Center for the free use of Geoscience Laser Altimeter System data and the Consortium for Spatial Information for distributing Shuttle Radar Topography Mission data.

REFERENCES

[1] P. Gong, G. S. Biging, S. Lee, X. Mei, Y. Sheng, R. Pu, B. Xu, K. P. Schwarzr, and M. Mostafa, "Photo ecometrics for forest inventory," *Geogr. Inf. Sci.*, vol. 5, no. 1, pp. 9–14, 1999.

[2] A. T. Moles, D. I. Warton, L. Warman, N. G. Swenson, S. W. Laffan, A. E. Zanne, A. Pitman, F. A. Hemmings, and M. R. Leishman, "Global patterns in plant height," *J. Ecol.*, vol. 97, no. 5, pp. 923–932, Sep. 2009.

[3] M. A. Lefsky, "A global forest canopy height map from the Moderate Resolution Imaging Spectroradiometer and the Geoscience Laser Altimeter System," *Geophys. Res. Lett.*, vol. 37, no. 15, pp. L15401-1–L15401-5, Aug. 2010.

[4] M. Simard, N. Pinto, J. B. Fisher, and A. Baccini, "Mapping forest canopy height globally with spaceborne lidar," *J. Geophys. Res., Biogsci.*, vol. 116, no. G4, pp. G04021-1–G04021-12, Dec. 2011.

[5] A. C. Brenner, H. J. Zwally, C. R. Bentley, B. M. Csathó, D. J. Harding, L. J. Minster, J. L. Roberts, R. H. Saba, and D. Thomas, Derivation of Range and Range Distribution From Laser Pulse, Feb. 2012. [Online]. Available: http://www.csr.utexas.edu/glas/atbd.html

[6] Q. Chen, "Retrieving vegetation height of forests and woodlands over mountainous areas in the Pacific Coast region using satellite laser altimetry," *Remote Sens. Environ.*, vol. 114, no. 7, pp. 1610–1627, Jul. 2010.

[7] J. Rosette, P. North, and J. Suarez, "Vegetation height estimates for a mixed temperate forest using satellite laser altimetry," *Int. J. Remote Sens.*, vol. 29, no. 5, pp. 1475–1493, Mar. 2008.

[8] H. Wu and Y. Xing, "Wavelet transform and its application to ICESat—GLAS full waveform data," in *Proc. Int. Symp. Intell. Inf. Process. Trusted Comput.*, 2010, pp. 373–377.

[9] C. Wang, F. Tang, L. Li, G. Li, F. Cheng, and X. Xi, "Wavelet analysis for ICESat/GLAS waveform decomposition and its application in average tree height estimation," *IEEE Geosci. Remote Sci. Lett.*, vol. 10, no. 1, pp. 115–119, Jan. 2013.

[10] M. E. Miller, M. Lefsky, and Y. Pang, "Optimization of geoscience laser altimeter system waveform metrics to support vegetation measurements," *Remote Sens. Environ.*, vol. 115, no. 2, pp. 298–305, Feb. 2011.

[11] M. A. Lefsky, M. Keller, Y. Pang, P. B. De Camargo, and M. O. Hunter, "Revised method for forest canopy height estimation from Geoscience Laser Altimeter System waveforms," *J. Appl. Remote Sens.*, vol. 1, no. 1, p. 013537, Jun. 2007.

[12] M. A. Lefsky, D. J. Harding, M. Keller, W. B. Cohen, C. C. Carabajal, F. D. B. Espirito-Santo, and M. O. Hunter, "Estimates of forest canopy height and aboveground biomass using ICESat," *Geophys. Res. Lett.*, vol. 32, no. 5, p. L22S02, Mar. 2005.

[13] S. O. Los, J. A. B. Rosette, N. Kljun, P. R. J. North, J. C. Suárez, C. Hopkinson, R. A. Hill, L. Chasmer, E. van Gorsel, C. Mahoney, and J. A. J. Berni, "Vegetation height products between 60° S and 60° N from ICESat GLAS data," *Geosci. Model Dev. Discuss.*, vol. 4, no. 3, pp. 2327–2363, Sep. 2011.

[14] Y. Pang, M. Lefsky, H. E. Andersen, M. E. Miller, and K. Sherrill, "Validation of the ICEsat vegetation product using crown-area-weighted mean height derived using crown delineation with discrete return lidar data," *Can. J. Remote Sens.*, vol. 34, no. S2, pp. 471–484, Nov. 2008.

[15] S. Lee, W. NiMeister, W. Yang, and Q. Chen, "Physically based vertical vegetation structure retrieval from ICESat data: Validation using LVIS in White Mountain National Forest, New Hampshire, USA," *Remote Sens. Environ.*, vol. 115, no. 11, pp. 2776–2785, Nov. 2011.

[16] P. Gong, J. Wang, L. Yu, Y. Zhao, Y. Zhao, L. Liang, Z. Niu, X. Huang, H. Fu, S. Liu, C. Li, X. Li, W. Fu, C. Liu, Y. Xu, X. Wang, Q. Cheng, L. Hu, W. Yao, H. Zhang, P. Zhu, Z. Zhao, H. Zhang, Y. Zheng, L. Ji, Y. Zhang, H. Chen, A. Yan, J. Guo, L. Yu, L. Wang, X. Liu, T. Shi, M. Zhu, Y. Chen, G. Yang, P. Tang, B. Xu, C. Giri, N. Clinton, Z. Zhu, J. Chen, and J. Chen, "Finer resolution observation and monitoring of global land cover: First mapping results with Landsat TM and ETM + data," *Int. J. Remote Sens.*, vol. 34, no. 7, pp. 2607–2654, Apr. 2013.

[17] X. Wang, X. Cheng, P. Gong, H. Huang, Z. Li, and X. Li, "Earth science applications of ICESat/GLAS: A review," *Int. J. Remote Sens.*, vol. 32, no. 23, pp. 8837–8864, Dec. 2011.

[18] J. B. Blair, D. L. Rabine, and M. A. Hofton, "The laser vegetation imaging sensor: A medium-altitude, digitisation-only, airborne laser altimeter for mapping vegetation and topography," *ISPRS J. Photogramm. Remote Sens.*, vol. 54, no. 2/3, pp. 115–122, Jul. 1999.

[19] A. Jarvis, H. Reuter, A. Nelson, and E. Guevara, CGIAR-CSI SRTM 90m Database; Hole-filled SRTM for the globe Version 4 2008. [Online]. Available: http://srtm.csi.cgiar.org

[20] A. Savitzky and M. J. E. Golay, "Smoothing and differentiation of data by simplified least squares procedures," *Anal. Chem.*, vol. 36, no. 8, pp. 1627–1639, Jul. 1964.

[21] J. Chen, P. Jönsson, M. Tamura, Z. Gu, B. Matsushita, and L. Eklundh, "A simple method for reconstructing a high-quality NDVI time-series data set based on the Savitzky–Golay filter," *Remote Sens. Environ.*, vol. 91, no. 3/4, pp. 332–344, Jun. 2004.

[22] J. Steinier, Y. Termonia, and J. Deltour, "Smoothing and differentiation of data by simplified least square procedure," *Anal. Chem.*, vol. 44, no. 11, pp. 1906–1909, Sep. 1972.
[23] P. Gong, Z. Li, H. Huang, G. Sun, and L. Wang, "ICEsat GLAS data for urban environment monitoring," *IEEE Trans. Geosci. Remote Sens.*, vol. 49, no. 3, pp. 1158–1172, Mar. 2011.
[24] J. L. Devore, *Probability and Statistics for Engineering and the Sciences*. Boston, MA, USA: Duxbury Press, 2011.
[25] G. Sun, K. Ranson, D. Kimes, J. Blair, and K. Kovacs, "Forest vertical structure from GLAS: An evaluation using LVIS and SRTM data," *Remote Sens. Environ.*, vol. 112, no. 1, pp. 107–117, Jan. 2008.
[26] G. Sun and K. J. Ranson, "Modeling lidar returns from forest canopies," *IEEE Trans. Geosci. Remote Sens.*, vol. 38, no. 6, pp. 2617–2626, Nov. 2000.
[27] Y. Pang, Z. Li, M. Lefsky, G. Sun, and X. Yu, "Model based terrain effect analyses on ICEsat GLAS waveforms," in *Proc. IEEE Int. Geosci. Remote Sens. Symp.*, 2006, pp. 3232–3235.

Xiaoyi Wang received the B.S. degree in remote sensing science and technology from Wuhan University, Wuhan, China, in 2010. She is currently working toward the Ph.D. degree in cartography and geographic information systems in the University of the Chinese Academy of Sciences, Beijing, China.

Her primary research interests include forest height and structure extraction with lidar data.

Huabing Huang received the B.S. degree in soil and water conservation and desertification control from Northwest Agriculture and Forestry University, Yangling, China, in 2002 and the M.S. and Ph.D. degrees in cartography and geographic information systems from the Graduate School of the Chinese Academy of Sciences (CAS), Beijing, China, in 2005 and 2008, respectively.

He is currently an Associate Research Scientist with the State Key Laboratory of Remote Sensing, jointly sponsored by the Institute of Remote Sensing and Digital Earth, CAS, and Beijing Normal University, Beijing. His research activities focus on LiDAR applications in forest and polar regions.

Peng Gong received the B.S. and M.S. degrees in geography from Nanjing University, Nanjing, China, in 1984 and 1986, respectively, and the Ph.D. degree in geography from the University of Waterloo, Waterloo, ON, Canada, in 1990.

He was a Research Scientist with the Institute for Space and Terrestrial Science, North York, ON, Canada, and an Assistant Professor with the Department of Geomatics Engineering, University of Calgary, AB, Canada, before joining the Department of Environmental Science, Policy and Management, University of California, Berkeley, CA, USA, in 1994, where he became a Full Professor in 2001. He was the Advisor to the Ministry of Science and Technology of China in 2004–2006. He was the Founding Director of the International Institute for Earth System Science, Nanjing University, between 2000 and 2007 and the Founding Director of the State Key Laboratory of Remote Sensing Science, Chinese Academy of Sciences, and Beijing Normal University, Beijing, China, between 2004 and 2010. He became the Director of the Center for Earth System Science, Tsinghua University, Beijing, in 2010. He has authored/coauthored six books and over 400 publications, including more than 300 journal articles in the field of remote sensing, geography, and environmental science. His current interest is remote sensing, global environmental change, and public health.

Prof. Gong was the recipient of a number of honors and awards, including the Outstanding Contribution Award in Remote Sensing from the Association of American Geographers in 2008 and the Talbert Abrams Grand Award from the American Society for Photogrammetry and Remote Sensing in 1994.

Caixia Liu received the B.S. degree in geomatics engineering from Central South University, Changsha, China, in 2006 and the M.S. degree in signal and information processing from the Graduate School of the Chinese Academy of Sciences (CAS), Beijing, China, in 2009. She is currently working toward the Ph.D. degree in cartography and geographic information systems in the University of CAS.

She is also an Assistant Research Scientist with the State Key Laboratory of Remote Sensing, jointly sponsored by the Institute of Remote Sensing and Digital Earth, CAS, and Beijing Normal University, Beijing. Her current research interests focus on mapping forest height from multisensor data and inland water level monitoring using spaceborne lidar.

Congcong Li received the B.S. degree in forestry from Beijing Forestry University, Beijing, China, in 2009. She is currently working toward the Ph.D. degree in global environment change in the College of Global Change and Earth System Science, Beijing Normal University, Beijing.

Her current research interest is forest classification.

Wenyu Li received the B.S. degree from Tongji University, Shanghai, China, in 2010. He is currently working toward the M.S. degree in cartography and geographic information systems from the University of Chinese Academy of Sciences, Beijing, China.

His current research interest is shoreline change.